ACTA IMEKO
ISSN: 2221-870X
March 2025, Volume 14, Number 1, 1 - 10

Methodology for assessing the accuracy of a measuring instrument for the ion concentration using its measurement model

Oleksandr Vasilevskyi[1]

[1] *Walker Department of Mechanical Engineering, The University of Texas at Austin, 204 E Dean Keeton Street, Austin, TX 78712, USA*

ABSTRACT
To analyze the metrological characteristics of measuring instruments, it was proposed to expand the conversion equation into a Taylor series. The components of this series yield equations that describe the instrument's sensitivity as well as its additive and multiplicative errors. Additionally, a mathematical model is introduced, allowing the conversion of these additive and multiplicative errors into measurement uncertainty. The proposed models were tested using a measurement model for ion concentration based on ion-selective electrodes. The measurement accuracy assessment methodology demonstrated that the expanded uncertainty of ion concentration measurements ranges from ± 0.101 pX to ± 0.204 pX, depending on the measurement range. Measurements performed at the beginning of the measurement range exhibit lower values of expanded uncertainty, while measurements conducted at the upper measurement range show slightly higher values of expanded uncertainty.

Section: RESEARCH PAPER

Keywords: ion concentration; measurement means; metrological characteristics; measurement model; Taylor series; measurement uncertainty

Citation: O. Vasilevskyi, Methodology for assessing the accuracy of a measuring instrument for the ion concentration using its measurement model, Acta IMEKO, vol. 14 (2025) no. 1, pp. 1-10. DOI: 10.21014/actaimeko.v14i1.1938

Section Editor: Leonardo Iannucci, Politecnico di Torino, Italy

Received September 20, 2024; **In final form** November 27, 2024; **Published** March 2025

Corresponding author: Oleksandr Vasilevskyi, e-mail: oleksandr.vasilevskyi@austin.utexas.edu

1. INTRODUCTION

The study of measurement accuracy for ion concentration in substances, based on different principles of instrument design, is a relevant task aimed at enhancing the reliability of measurements. One approach to improving measurement reliability is by reducing measurement errors through advancements in ion concentration measurement methods. According to various sources [1]-[7], the most commonly used physic and chemical methods for determining ion activity (concentration) include amperometry, high-frequency titration, spectrophotometry, chronoconductometry, and ionometry.

The objective of this paper is to develop a methodology for assessing the accuracy of measuring instruments by calculating analytical expressions for the additive and multiplicative errors present in models used to measure ion concentrations of humus components in soil. This is achieved by expanding the measurement instrument transformation equation into a Taylor series. As is known from works [8]-[12], the main accuracy characteristics of measurement instruments include sensitivity, additive and multiplicative errors, and uncertainty. It is also necessary that the mathematical tools used in measuring instrument research allow us to easily derive equations for estimating basic accuracy characteristics. Therefore, it would be beneficial to develop a generalized mathematical framework for studying the metrological characteristics of measuring instruments, which can be readily expressed in terms of measurement uncertainties. This approach involves using a model equation that describes the operation of the measuring instrument. The model equation is expanded into a Taylor series [13], from which mathematical models for the additive and multiplicative errors of the instrument are derived. The mathematical models of measuring means errors make it possible to study the characteristics of their changes depending on the measurement range and other values of the influencing quantities. The characteristics of the errors of measuring means obtained in this way are proposed to be recalculated into characteristics of measurement uncertainty. For this purpose, a methodology has been developed for converting the error characteristics into uncertainty characteristics, which is described in detail in this work.

2. METHOD AND MEASUREMENT MODEL

Potentiometry is an electrochemical method based on measuring the potential difference between two electrodes immersed in the studied environment. By determining the electrode potential, it is possible to assess the activity (concentration) of particles or monitor changes in this activity during a reaction. The active part of the selective electrode forms a boundary between the electrode's sensitive element and the studied environment, where ion exchange occurs. This leads to the establishment of thermodynamic equilibrium, in which the electrochemical potentials of the ions on both sides of the boundary are equal. These potentials are determined by the activity of the ions being studied, with the ion activity in the sensitive element remaining constant and varying in the studied environment. When applying an equation that relates the potential difference across the boundary to the activity of specific ions in the environment, the Nernst equation is formulated as follows [14]:

$$\Delta U = U_0 + \frac{2.3\ R\ T}{n_i\ F} \lg a_i\ , \tag{1}$$

where ΔU - is the potential difference between the ion – selective and auxiliary electrodes (mV); U_0 - is the value of the potential in the initial point of the measuring range (mV); R - is the universal molar gas constant; T - is the absolute temperature of the studied environment; n_i – is the charge of the ith ion; F - is the Faraday constant, a_i – is the activity of the ith ion in the studied environment [15]-[18].

General potential difference between the two ends of the circuit is described by the expression [15], [16]:

$$\Delta U = \left(E_r + U_0 + \frac{2.3\ R\ T}{n_i\ F} \lg a_i\right) - \left(E_r{}' + U_0 + \frac{2.3\ R\ T}{n_i\ F} \lg a_i{}'\right). \tag{2}$$

Having grouped the constant values, we obtain the graduation voltage $U_0{}'$, which is determined by the selection of the count point:

$$U_0{}' = E_r - \frac{2.3\ R\ T}{n_i\ F} \lg a_i{}' - E_r{}'\ . \tag{3}$$

In expression (3) it is also necessary to take into account the potential of the electrode bridge and asymmetry potential of the sensitive element, as a result we obtain:

$$\Delta U = U_0{}' + \frac{2.3\ R\ T}{n_i\ F} \lg a_i\ . \tag{4}$$

Ion-selective electrodes generate a signal determined by the activity of the ions, which, at a constant temperature, depends on factors such as the concentration of the studied ions, their charge (electrovalence), size, and the nature and concentration of other ions present in the environment [19]-[21]. The characteristics of the potential difference of ion-selective electrodes, as described by the transformation equation (4), vary depending on the range of chemical substances' charges, which include both negatively and positively charged ions. These characteristics are illustrated in Figure 1. The Maple software environment was utilized to construct all characteristics of the variation in measured and additional quantities based on the proposed transformation equations.

In ionometry, the concentration of ions is expressed in terms of *pX* values, which are related to the ion activity by the following equation:

$$pX_i = -\lg a_i\ . \tag{5}$$

Substituting the expression (5) in the transformation equation of ion selective electrodes (4), we obtain a linearized transformation equation:

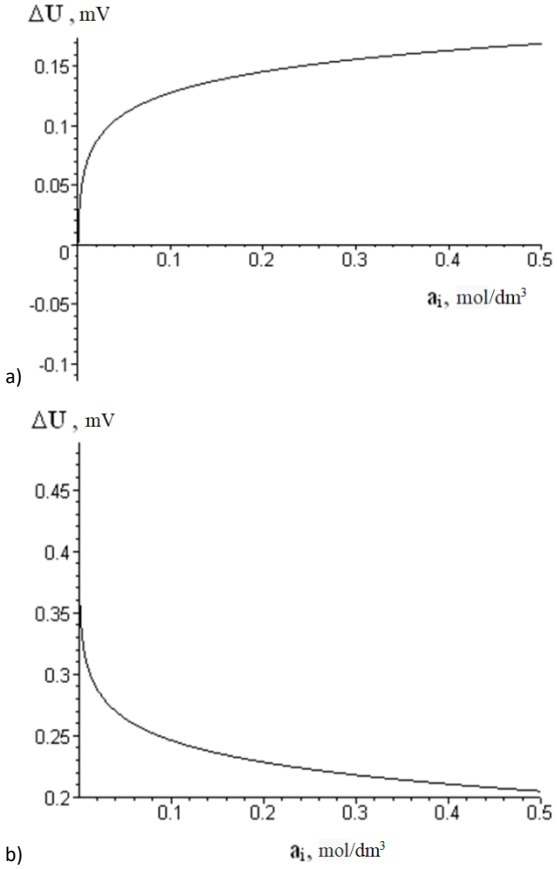

Figure 1. Characteristics of the potential differences change: a) - at positively charged ions; b) - at negatively charged ions.

$$\Delta U = U_0{}' - \frac{2.3\ R\ T}{n_i\ F} pX_i\ . \tag{6}$$

To improve the accuracy of measuring ion concentration in chemical substances, it is suggested to simultaneously measure the temperature of the environment along with the ion concentration. Using the measured temperature, the potential difference ΔU of the ion-selective electrodes can be calculated. For this purpose, the steepness coefficient $S = 2.3\ R\ T/F$ in equation (6) is replaced with an expression $\alpha\ (273.15 + t)$ that accounts for temperature variations. This modification results in a linearized transformation equation for the ion-selective electrode, which has the following form:

$$\Delta U = U_0{}' - \frac{\alpha\ (273.15 + t)}{n_\mathrm{a}} pX_i\ , \tag{7}$$

where α is temperature coefficient of the steepness S, that equals 198.4 × 10^{-3}/K; t is the temperature (in °C) of the environment being analysed [14], [22], [23].

Figure 2 illustrates the static characteristics of the linearized transformation Equation (7), which includes the measured temperature of the examined environment.

To assess the influence of temperature, a key factor in the transformation Equation (7), on ion concentration measurements, we examined the errors resulting from a 1 K temperature variation. The reference theoretical temperature, assumed without additional measurements, is 25 °C. We calculated the impact of a 1 K deviation from this baseline using a mathematical model for the relative error:

$$\delta U = \frac{[t_d - t]\dfrac{\alpha \cdot pX_i}{n_\mathrm{a}}}{U_0{}' - \dfrac{\alpha\ (273{,}15 + t_d)}{n_\mathrm{a}}\ pX_i} \cdot 100\ \%\ , \tag{8}$$

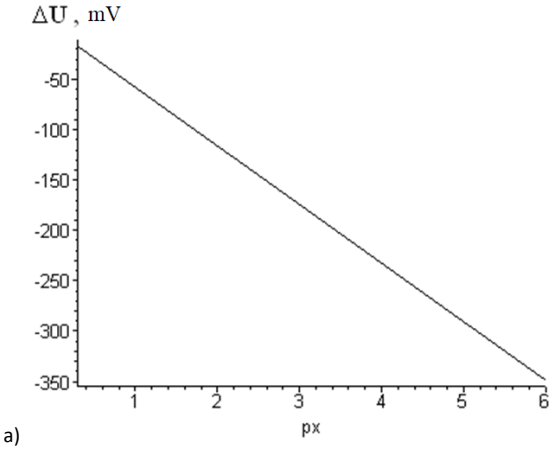

a)

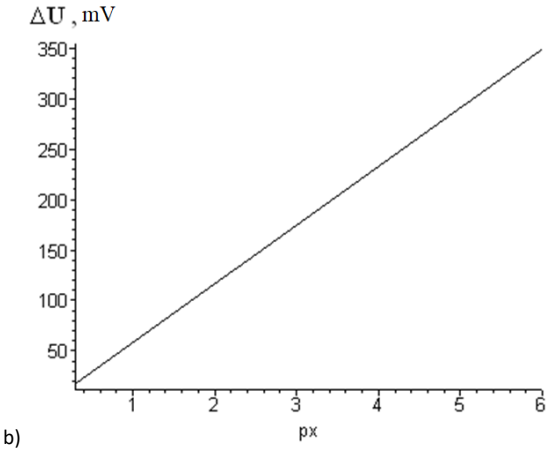

b)

Figure 2. The static characteristics of ion-selective electrodes at a temperature of 20 °C are depicted as follows: a) For positively charged ions; b) For negatively charged ions.

where t is the theoretical value of the temperature that equals the calibration temperature of the ion selective electrode 25 °C; t_d is the real value of the studied environment temperature, which deviates from the theoretical by 1 K.

Figure 3 illustrates the relative error characteristic caused by a 1 K deviation from the theoretically accepted temperature value (25 °C) across the entire measurement range for negatively charged ions. Similarly, Figure 4 shows the relative error characteristic for positively charged ions.

Based on the error analysis conducted (as shown in Figure 3 and Figure 4), it is evident that temperature significantly affects ion

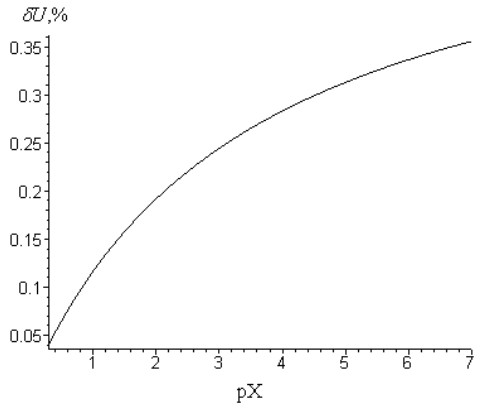

Figure 3. Characteristic of the relative measurement error change for negatively charged ions resulting from a 1 K temperature deviation.

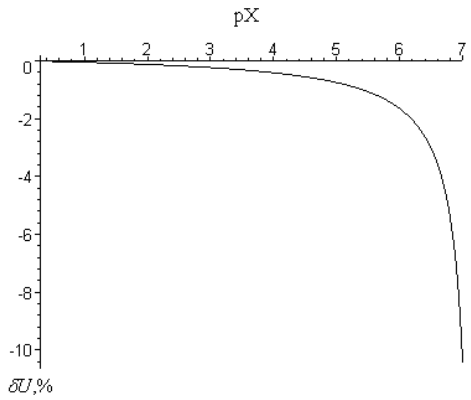

Figure 4. Characteristic of the relative measurement error change for positively charged ions concentration resulting from a 1 K temperature deviation.

concentration measurements. The error introduced by a deviation of the actual temperature from the theoretical value, which is used as the default calibration temperature, is 0.36 % / K for negatively charged ions. For positively charged ions, the error is 10.4 % / K at a low measurement range of 7 pX. Therefore, the execution of direct temperature measurements can significantly enhance the accuracy of ion concentration measurements. The linearized transformation equation (7), which includes additional temperature measurements, allows for high-accuracy studies of ion concentrations. As the research indicates (Figure 3), the temperature measurement channel should have an error of less than ±0.05 % (or absolute temperature limits ± (0.15 K + 0.002 t)) for the lower measurement range of 0.3 pX to effectively account for a 1 °C temperature change.

It is also known that when measuring the activity of primary ions according to the Nikolsky equation [24], the accuracy of the measurement (electrode potential) is influenced by the presence of extraneous ions:

$$\Delta U = U_0{}' + \frac{\alpha\,(273.15 + t)}{n_\mathrm{a}} \lg(a_\mathrm{A} + K_\mathrm{c}\, a_\mathrm{B})\,, \tag{9}$$

where a_A is the activity of the main ions that are to be measured; a_B is the activity of foreign (interfering) ions; K_c is selectivity coefficient.

Studies on the impact of foreign ions on the measurement of primary ion activity were conducted in [6], [25] and are not addressed in this work. These studies utilized ion-selective electrodes to measure the activity of ammonium nitrogen, potassium, nitrate nitrogen, and fluoride. It is well known that the ion-selective electrode is designed to measure the activity of certain ions even in the presence of 10-100 times more foreign (interfering) ions [26]. The selectivity coefficient of an ion-selective electrode, which depends on the nature of the ions being measured, is determined experimentally to improve calibration accuracy. Experimental results indicated that the selectivity coefficient is significantly less than one for the studied ions, meaning that the interfering ions do not significantly impact the accuracy of the primary ion measurements. Consequently, the measurement model does not account for interfering ions, assuming that all used ion-selective electrodes are sufficiently selective for the primary ions. However, if experimental data indicate that interfering ions significantly affect the electrode potential (i.e., when the selectivity coefficient is equal to or exceeds one), corrections are made to account for their influence on the measurement of primary ion activity. Various principles of secondary measurement conversion, including analog-to-digital conversion with successive approximation, time-pulse conversion, and voltage-to-frequency conversion, were also investigated [6], [11]. The proposed means of measuring ion concentration is intended to control the humus components in soil with improved metrological characteristics. In this case, the means for measuring ion concentration consists of ion-selective electrodes, a reference electrode, a secondary measuring transducer, and a temperature-measuring channel. As a

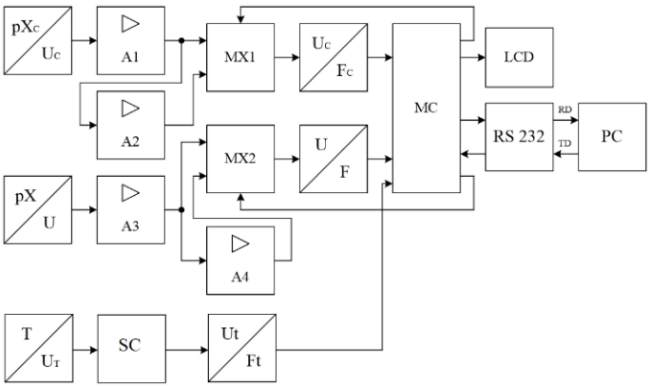

Figure 5. The diagram of the digital transducer for ion concentration measurement, built using voltage-to-frequency converters.

result of research, it was found that, together with ion-selective electrodes and a reference electrode, it is best to use the principle of voltage-to-frequency conversion as a secondary measuring transducer [11], since such a voltage-to-frequency converter (AD7742) shows the highest accuracy even with insignificant nonlinearity of the output characteristic (0.012 %). The block diagram of the measurement system, shown in Figure 5, includes [11]: the ion-selective converter (pX/U), reference electrode (pXC/UC), two operational amplifiers in each measurement channel (MC) for measuring both positive and negative *pX* values (A1 – A4), multiplexers (MX1 and MX2), voltage-to-frequency converters (VFC) for converting the potentials of the reference electrode (UC/FC) and ion-selective electrode (U/F) into frequency, the microcontroller (MC), the liquid crystal display (LCD), the voltage levels converter (RS232) for data transfer to a computer (PC). The temperature measurement channel includes the thermosensitive converter, the scale converter (SC), and the voltage-to-frequency converter.

Considering the equation for converting ion concentration into voltage (Equation 7), which governs the operation of the ion-selective electrode, and the conversion function of the secondary voltage-to-frequency converter (AD7742), we can derive a combined conversion function that models the process of measuring ion concentration using the proposed high-precision instrument:

$$N_{\mathrm{U/F}} = \frac{U_{\max}\,\tau\,f_0}{(U_0{}' - \alpha\,(273.15 + t)\,n_{\mathrm{a}}^{-1}\,pX_i)\,k}, \tag{10}$$

where $U_{\max}$ – is the value of the reference voltage of VFC (10 V); $\tau = RS$ – constant of VFC time, used for setting the full-scale output frequency of the quartz-crystal resonator of the microcontroller (R = 1 kOhm, C = 47 mF); f_0 – is the frequency of the quartz-crystal resonator of the microcontroller (20 MHz); α – is temperature coefficient of steepness S, that equals $198.4 \times 10^{-3}/K$; t – is the temperature (in °C) of the environment being analysed; $U_0{}'$ – the graduation voltage, which is determined by the selection of the reference point; pX_i – the concentration of ions; n_{a} – is the ion charge; k - is the amplification factor of the operational amplifier [6], [27].

Figure 6 presents the characteristics of the output signal variations of the measuring instrument, represented as a binary decimal code $N_{\mathrm{U/F}}$, in relation to the input measurement range (ion concentration pX_i) and the charge of the ions (positive or negative). These characteristics reveal that the transformation function of the instrument is nonlinear. Nevertheless, despite this nonlinearity, the VFC exhibits an exceptionally low level of nonlinearity across a broad frequency range, with deviations staying below 0.012 % [28].

Using the measurement model (10), analytical dependencies were derived for studying additive and multiplicative errors, the method for obtaining which is described in detail in Section 3.

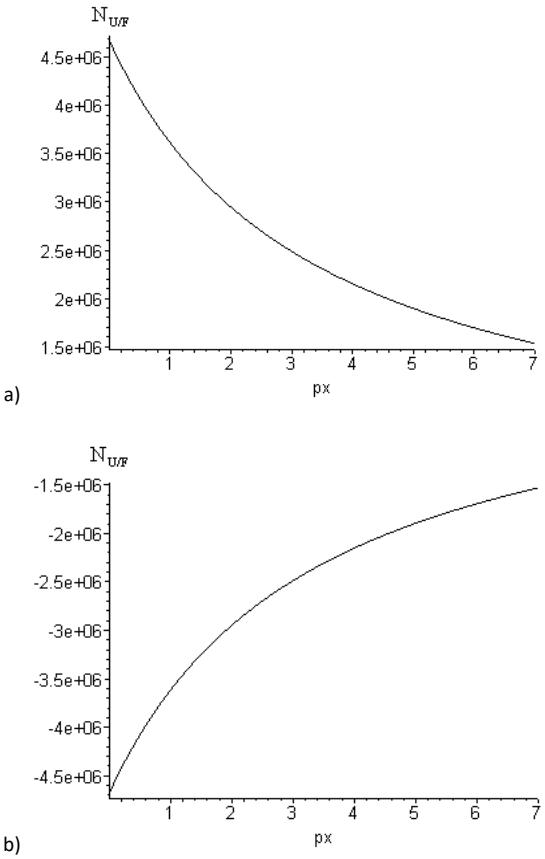

Figure 6. Static characteristics of the ion concentration measuring instrument are shown as follows: a) when measuring negatively charged ions; b) when measuring positively charged ions.

3. ADDITIVE AND MULTIPLICATIVE ERRORS

Under the operating conditions of the measurement means, the ion concentration is functionally converted from the input-measured value pX_i into a pulse count (binary decimal code $N_{\mathrm{U/F}}$). In addition to the measured input value pX_i, various influencing factors affect the conversion process. These include parameters that are directly linked to the input value and introduce non-informative components into the conversion. An analysis of the derived measurement model (10) reveals that the conversion of the informative parameter pX_i into the output signal is impacted by numerous factors. However, since most of these factors remain constant, and temperature is one of the key variables when measuring ion concentration, we will focus on examining the role of temperature as an influencing factor on the informative parameter.

To derive analytical expressions for the key metrological characteristics of the measurement means for ion concentration, we can expand our measurement model (10) using Taylor's Series, resulting in the following dependencies [13], [29]:

$$\begin{aligned} N_{\mathrm{U/F}} = N_{\mathrm{U/F}}\big|_0 + \left[\frac{\partial N_{\mathrm{U/F}}}{\partial pX_i}\right]_0 pX_i + \frac{1}{2}\left[\frac{\partial^2 N_{\mathrm{U/F}}}{\partial pX_i{}^2}\right]_0 pX_i{}^2 \\ + + \frac{1}{6}\left[\frac{\partial^3 N_{\mathrm{U/F}}}{\partial pX_i{}^3}\right]_0 pX_i{}^3 + \ldots + \left[\frac{\partial^2 N_{\mathrm{U/F}}}{\partial pX_i\,\partial t}\right]_0 pX_i\,\Delta t \\ + \left[\frac{\partial N_{\mathrm{U/F}}}{\partial t}\right]_0 \Delta t + + \frac{1}{2}\left[\frac{\partial^2 N_{\mathrm{U/F}}}{\partial t^2}\right]_0 \Delta t^2 + \cdots . \end{aligned} \tag{11}$$

The nominal conversion factor, or sensitivity, of the ion concentration measurement means is determined by the following expression:

$$S_{\mathrm{U/F}} = \frac{\partial N_{\mathrm{U/F}}}{\partial pX_i} = \frac{U_{\max}\,\tau\,f_0\,\alpha\,(273.15+t)}{k\,n_{\mathrm{a}}\left(U_0' - \dfrac{\alpha\,(273.15+t)}{n_{\mathrm{a}}}pX_i\right)^2}. \tag{12}$$

The changes in sensitivity across the conversion range of the input measured value pX_i are given by the derivative of the second-order equation of the measurement model (10):

$$S'_{\mathrm{U/F}} = \frac{\partial^2 N_{\mathrm{U/F}}}{2\,\partial pX_i^2} = \frac{U_{\max}\,\tau\,f_0\,\alpha^2(273.15+t)^2}{k\,n_{\mathrm{a}}^2\left(U_0' - \dfrac{\alpha\,(273.15+t)}{n_{\mathrm{a}}}pX_i\right)^3}. \tag{13}$$

The second derivative concerning sensitivity in the range of transformation of the input measured value pX_i is determined by the following formula:

$$\frac{\partial S'_{\mathrm{U/F}}}{\partial pX_i} = \frac{\partial^3 N_{\mathrm{U/F}}}{6\,\partial pX_i^3} = \frac{U_{\max}\,\tau\,f_0\,\alpha^3(273.15+t)^3}{2\,k\,n_{\mathrm{a}}^3\left(U_0' - \dfrac{\alpha\,(273.15+t)}{n_{\mathrm{a}}}pX_i\right)^4}. \tag{14}$$

The influence coefficients of the influential quantity t on the output parameter $N_{\mathrm{U/F}}$ of the measurement model (10) are calculated using the following formulas:

$$\beta_{0t} = \frac{\partial N_{\mathrm{U/F}}}{\partial t} = \frac{U_{\max}\,\tau\,f_0\,\alpha}{k\,n_{\mathrm{a}}\left(U_0' - \dfrac{\alpha\,(273.15+t)}{n_{\mathrm{a}}}pX_i\right)^2}pX_i \tag{15}$$

$$\beta_{0t}{}' = \frac{\partial^2 N_{\mathrm{U/F}}}{2\,\partial t^2} = \frac{U_{\max}\,\tau\,f_0\,\alpha^2}{k\,n_{\mathrm{a}}^2\left(U_0' - \dfrac{\alpha\,(273.15+t)}{n_{\mathrm{a}}}pX_i\right)^3}pX_i\,. \tag{16}$$

The coefficient of the combined influence of the informative parameter pX_i and the influential value t (temperature) on the nominal sensitivity $S_{\mathrm{U/F}}$ of the measuring conversion is determined by the following expression

$$\alpha_{0t} = \frac{\partial^2 N_{\mathrm{U/F}}}{\partial pX_i\,\partial t} = \frac{2\,U_{\max}\,f_0\,\tau\,\alpha^2(273.15+t)\,pX_i}{k\,n_{\mathrm{a}}^2\left(U_0' - \dfrac{\alpha\,(273.15+t)}{n_{\mathrm{a}}}pX_i\right)^3} + \frac{U_{\max}\,f_0\,\tau\,\alpha}{k\,n_{\mathrm{a}}\left(U_0' - \dfrac{\alpha\,(273.15+t)}{n_{\mathrm{a}}}pX_i\right)^2}. \tag{17}$$

The reference transformation function of the measuring model of ion concentration is determined from the expansion of the Equation (10) into a Taylor series, incorporating the obtained expressions (12) – (14), and is given by the following formula

$$N_{\mathrm{U/Fref}} = S_{\mathrm{U/F}}\,pX_i + S'_{\mathrm{U/F}}\,pX_i^2 + \frac{\partial S'_{\mathrm{U/F}}}{\partial pX_i}pX_i^3\,. \tag{18}$$

The absolute error of the nonlinearity of the reference transformation function (18) can be found using the following expression:

$$\Delta N_{\mathrm{U/Fref}} = S'_{\mathrm{U/F}}\,(pX_i - pX_{i\mathrm{ref}})^2 + \frac{\partial S'_{\mathrm{U/F}}}{\partial pX_i}(pX_i - pX_{i\mathrm{ref}})^3\,, \tag{19}$$

where $pX_{i\mathrm{ref}}$ is the reference value of the ion concentration.

The characteristic of the change in the absolute error of nonlinearity (19) of the reference transformation function when the measured value of the ion concentration pX_i deviates from the reference value of the ion concentration $pX_{i\mathrm{ref}}$ by 0.1 (pX) is plotted in Figure 7.

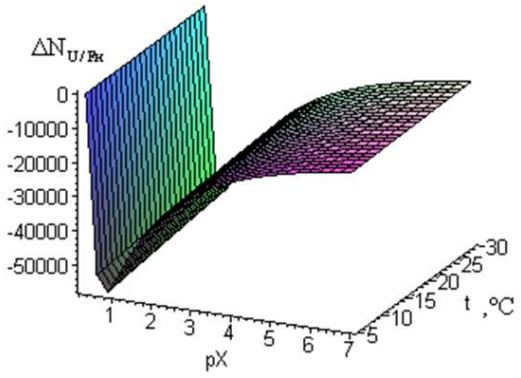

Figure 7. The absolute error of the nonlinearity of the nominal conversion function.

Considering the maximum value of the absolute nonlinearity error (Figure 7), which is $\Delta N_{\mathrm{U/Fref}}$ = -5 × 10⁴ binary-decimal units (pulses) and the ion concentration measurement range, expressed in binary-decimal units (pulses) D = 4.5 × 10⁶ - 1.5 × 10⁶ = 3 × 10⁶ (Figure 6, a), it was determined the values of the relative nonlinearity of the ion concentration measuring mean, which is $\delta_{\mathrm{n}} = \left|\Delta N_{\mathrm{U/Fref}}\right|/D$ = 5 × 10⁴/(3 × 10⁶) = 0.017 within the ion concentration range of 0.3 pX to 7 pX.

Given that the static characteristic exhibits nonlinearity across the ion concentration measurement range from 0.3 pX to 7 pX (Figure 6), the nonlinearity error model (19) allows for the estimation of the maximum error and an analysis of its variation. The nonlinearity error variation (Figure 7) highlights the ranges where the error is most prominent and where it is minimized, as well as the effect of temperature on the nonlinearity of the static characteristic.

Figure 7 illustrates that temperature variations between 5 °C and 30 °C have a minimal effect on the nonlinearity of the static characteristic of the ion activity measurement device. Moreover, Figure 7 indicates that within the measurement range of 0.6 pX to 3 pX, the nonlinearity error is higher but does not exceed 0.017. In contrast, within the ranges of 0.3 pX to 0.6 pX and 3 pX to 7 pX, the nonlinearity error is approximately 2.5 times smaller. Consequently, measurements of ion concentration within these ranges will result in higher accuracy.

The absolute multiplicative error N_{m} of transformation under the conditions of temperature change $\Delta t = (t - t_{\mathrm{ref}})$ can be determined by the following formula:

$$\Delta N_{\mathrm{m}} = \left(\frac{2\,U_{\max}\,f_0\,\tau\,\alpha^2(273.15+t)\,pX_i}{k\,n_{\mathrm{a}}^2\left(U_0' - \dfrac{\alpha\,(273.15+t)}{n_{\mathrm{a}}}pX_i\right)^3} + \frac{k^{-1}\,n_{\mathrm{a}}^{-1}\,U_{\max}\,f_0\,\tau\,\alpha}{\left(U_0' - \dfrac{\alpha\,(273.15+t)}{n_{\mathrm{a}}}pX_i\right)^2}\right)pX_i\,\Delta t\,, \tag{20}$$

where t_{ref} in Δt is the reference temperature value (which was 20 °C).

The absolute additive error N_{a} of the transformation under conditions of a change in temperature $\Delta t = (t - t_{\mathrm{ref}})$ from the reference value t_{ref} can be determined by the expression:

$$\Delta N_{\mathrm{a}} = \frac{U_{\max}\,\tau\,f_0\,\alpha\,pX_i}{k\,n_a\left(U_0' - \dfrac{\alpha(273.15+t)}{n_{\mathrm{a}}}pX_i\right)^2}\Delta t + \frac{U_{\max}\,\tau\,f_0\,\alpha^2\,pX_i}{k\,n_{\mathrm{a}}^2\left(U_0' - \dfrac{\alpha\,(273.15+t)}{n_{\mathrm{a}}}pX_i\right)^3}\Delta t^2\,. \tag{21}$$

The characteristics of the changes in the obtained analytical dependencies of the multiplicative (20) and additive (21) errors of the

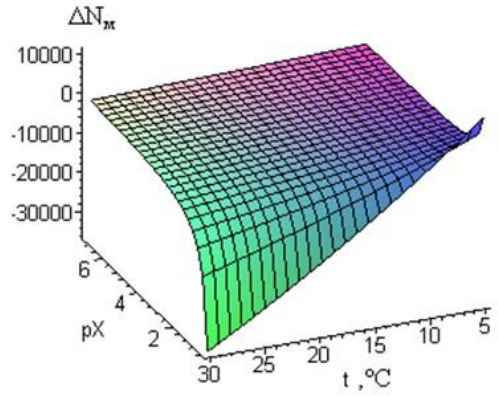

Figure 8. The absolute multiplicative error of ion concentration conversion under conditions of temperature change.

measuring channel for ion concentration are illustrated in Figure 8 and Figure 9, respectively.

The analysis of the multiplicative error, derived from model (20) and presented in Figure 8, reveals that temperature fluctuations have a considerable influence on the multiplicative error, particularly in the lower measurement range for ion concentration. Specifically, in the range of 0.3 pX to 0.6 pX, temperature variations significantly affect the multiplicative error. Figure 8 demonstrates that when the temperature decreases from 10 °C to 5 °C, the absolute multiplicative error increases sharply to +10,000 binary decimal units. On the other hand, as the temperature increases from 10 °C to 30 °C, the error becomes negative and progressively reaches -30,000 binary decimal units, especially at the lower ion concentrations (0.3 pX).

This shows that temperature changes can cause substantial variations in the multiplicative error of ion concentration measurements.

As illustrated in Figure 8 and Figure 9, the absolute multiplicative and additive errors of ion concentration exhibit their highest values when measuring at the beginning limits of the measurement range (0.3 pX) under conditions of temperature deviation Δt. The range of maximum deviation for both multiplicative and additive errors, due to changes in the influencing quantity t, is 3×10^4 pulses (Figure 8 and Figure 9). Given that the maximum output code is 4.5×10^6 pulses (Figure 6), this deviation corresponds to 0.67 % across the ion concentration range from 0.3 pX to 7 pX. In absolute terms, these errors equate to 0.047 pX each ($\Delta N_\mathrm{m} = 0.047$ pX and $\Delta N_\mathrm{a} = 0.047$ pX).

The examination of the additive error, based on the mathematical model (21) and depicted in Figure 9, reveals a notable influence of temperature on the error, especially within the lower measurement range of 0.3 pX to 0.6 pX. Specifically, a decrease in temperature from 10 °C to 5 °C results in a more negative additive error, reaching -10,000 binary decimal units. Conversely, an increase in temperature from 10 °C to 30 °C causes the additive error to become positive, rising to +30,000 binary decimal units. Despite these variations, the relative error remains within a 0.67 % margin. These effects are most prominent when measuring ion concentration at the start of the measurement range (0.3 pX). To reduce these additive and multiplicative errors in the lower range, it is essential to carefully measure the temperature of the sample. In practical applications, as demonstrated in Figure 5, the device was used at a temperature of 18 °C. To ensure precise measurements, it is recommended to avoid using the device in the lower measurement range, where sensitivity is more pronounced. Additionally, the research found that for negatively charged ions, the additive and multiplicative error behaviours follow the trends shown in Figure 8 and Figure 9, whereas for positively charged ions, these errors exhibit opposite signs.

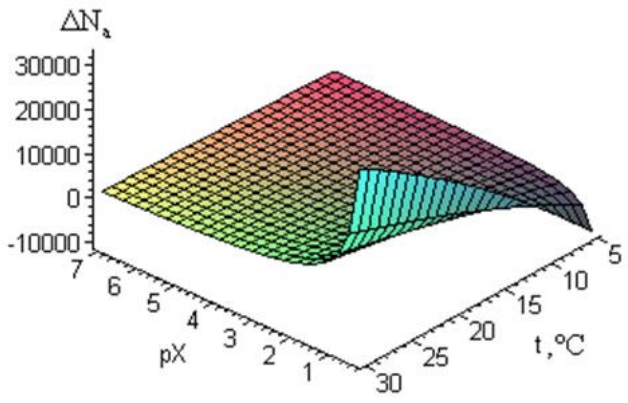

Figure 9. The absolute additive error of ion concentration conversion under conditions of temperature change.

To present the accuracy characteristics according to international standards for assessing measurement quality, it's crucial to have a methodology for converting the additive and multiplicative errors of measuring instruments into the instrumental component of type B uncertainty. This approach is proposed in the following 4th section of this article. It allows the results of error studies to be presented following international recommendations for expressing measurement uncertainties and ensures an accurate evaluation of the effectiveness of measurement results [30]-[34].

4. RESULTS AND MEASUREMENT UNCERTAINTY

4.1. Technique for converting errors into uncertainty

When applying the previously proposed methods to develop metrological models for additive and multiplicative errors, the challenge of converting these error components into measurement uncertainty in line with international standards arises [35]-[37]. To transform the additive and multiplicative errors of instruments into measurement uncertainty values, the following algorithm is suggested.

By applying the model equation (10) of the conversion of the measurement instrument to the Taylor series (11), we can derive the multiplicative (20) and additive (21) components of error in the measurement means. These components can generally be represented by the following expressions:

$$\Delta N_\mathrm{m} = \alpha_{0t}(pX - pX_\mathrm{ref})(\eta - \eta_\mathrm{ref}) \tag{22}$$

$$\Delta N_\mathrm{a} = \beta_{0t}(\eta - \eta_\mathrm{ref}) + \beta'_{0t}(\eta - \eta_\mathrm{ref})^2\,, \tag{23}$$

where N is the output value of the measurement instruments; pX is the measured input value; pX_ref is the reference value of the input value (the value that under normal conditions meets the requirements for calibration of the measurement instruments); η is the impact value; and η_ref is the reference value of the impact value [38].

If the nature of the error distribution law within specified limits is not known, international guidelines for estimating measurement uncertainty suggest assuming a uniform probability distribution for the error within an acceptable range. However, if the error distribution law is known within the boundaries of the quantities being studied, the uncertainty can be calculated based on the type of distribution law using established formulas as detailed in [34]-[39].

When there is no information available about the distribution laws of physical quantities, measurement uncertainty can be preliminarily estimated using the following formulas:

$$u(\Delta pX) = \frac{\Delta pX}{\sqrt{3}};\quad u(\Delta\eta) = \frac{\Delta\eta}{\sqrt{3}}, \tag{24}$$

where $\Delta pX = pX - pX_\mathrm{ref}$ is the deviation of the measured value pX from the reference value pX_ref; $\Delta\eta = \eta - \eta_\mathrm{ref}$ is the deviation of the

value of the influencing quantity η (for example, temperature t) from its reference value η_{ref}.

To estimate the combined Type B uncertainty using the values of additive and multiplicative errors, the following expression has been derived:

$$\begin{aligned} u_B^2 &= {\beta_{0t}}^2\, u^2(\Delta\eta) + (2\,\beta'_{0t}\,\Delta\eta)^2\, u^2(\Delta\eta) \\ &+ (\alpha_{0t}\,\Delta\eta)^2\, u^2(\Delta pX) + (\alpha_{0t}\,\Delta pX)^2\, u^2(\Delta\eta) \\ &= \frac{{\beta_{0t}}^2}{3}\Delta\eta^2 + \frac{(2\,\beta'_{0t}\,\Delta\eta)^2}{3}\Delta\eta^2 + \frac{(\alpha_{0t}\,\Delta\eta)^2}{3}\Delta pX^2 \\ &+ \frac{(\alpha_{0t}\,\Delta pX)^2}{3}\Delta\eta^2\,. \end{aligned} \tag{25}$$

This expression (25) is based on the rules for evaluating standard uncertainty through functional relationships outlined in [40], [41].

Thus, the methodology for converting the multiplicative and additive error components in measurement instruments involves determining the measured and influencing values based on the a priori information regarding type B uncertainties and calculating the instrumental variance component by Equation (25).

Considering the obtained numerical values of the Influence coefficients $\beta_{0t} = 2 \times 10^4\ \mathrm{K}^{-1}$ (15), $\beta_{0t}{}' = 70\ \mathrm{K}^{-2}$ (16), and the coefficient of compatible influence of the informative parameter $\alpha_{0t} = 7 \times 10^4\ \mathrm{K}^{-1}$ (17) in the Maple 13 software, along with the uncertainty values that arise when the temperature deviates by $\Delta\eta$ =1 K and the ion concentration by $\Delta pX = 0.1$ pX, we calculate the standard uncertainty using formula (25). Substituting the numerical values into (25), we obtain the uncertainty $u_{\mathrm{B}} = 12884$ binary-decimal pulses. By recalculating the obtained uncertainty in binary decimal pulses into the absolute value of the measured parameter pX ($u_{\mathrm{B}} = 7\ \mathrm{pX} \times 12884/(4.5 \times 10^6) = 0.02\ \mathrm{pX}$), we obtain the maximum value of the uncertainty of type B, which is u_{B} =0.02 pX in the ion concentration range of 0.3 pX to 7 pX, which is caused by the existence of additive and multiplicative errors when the temperature deviates by 1 K and the ion concentration by 0.1 pX from their reference values.

If the temperature deviates by $\Delta\eta$ =10 K from its reference (standardized) value (20 °C), then the uncertainty of ion concentration measurements caused by the existence of additive and multiplicative errors will be determined by formula (25) and will amount to $u_{\mathrm{B}} =$ 128844 binary-decimal pulses. The maximum value of the uncertainty of ion concentration measurements when recalculated to the measured value will be $u_{\mathrm{B}}(pX) = 7\ \mathrm{pX} \times 128844/(4.5 \times 10^6) = 0.2\ \mathrm{pX}$.

As calculations of the uncertainty of ion concentration measurements caused by the existence of additive and multiplicative errors show, the deviation of temperature from its reference value has a significant impact on the accuracy of the measurement results. Therefore, temperature value control is an important component of the ion concentration measurement procedure. Also, because of our study, we have demonstrated that type B uncertainty can be calculated based on the influence coefficients β_0, β'_0 and the combined influence of α_{0t}. These coefficients are used to determine multiplicative and additive errors and are derived by expansions of the transformation equation (measurement model) using the Taylor series. Knowing the values of these coefficients and the values of deviations from reference values of the influencing parameters, it is possible to determine what contribution their deviations make to the measurement uncertainty.

4.2. Results of the experiments performed

As a result of repeated experimental studies conducted to determine the ion concentration of humus components in solution using suitable ion-selective electrodes and a custom-developed measuring instrument, the following average ion concentration values were obtained, along with their associated type A measurement uncertainties [6], [41]:

- the average fluoride ion concentration was $\overline{pX}$ = 3.013 pF with a measurement uncertainty of type A of $u_{\mathrm{A}}(\overline{pX})$ = 0.003 pF;
- the average potassium ion concentration was $\overline{pX}$ = 1.905 pK with a measurement uncertainty of type A of $u_{\mathrm{A}}(\overline{pX})$ = 0.0026 pK;
- the average ammonium nitrogen ion concentration was $\overline{pX}$ = 5.345 $\mathrm{pNH_4}$ with a measurement uncertainty of type A of $u_{\mathrm{A}}(\overline{pX})$ = 0.0027 $\mathrm{pNH_4}$;
- the average nitrate nitrogen ion concentration was $\overline{pX}$ = 3.15 $\mathrm{pNO_3}$ with a measurement uncertainty of type A of $u_{\mathrm{A}}(\overline{pX})$ = 0.0028 $\mathrm{pNO_3}$;
- the average phosphate ion concentration was $\overline{pX}$ = 5.65 $\mathrm{pPO_3}$ with a measurement uncertainty of type A of $u_{\mathrm{A}}(\overline{pX})$ = 0.0039 $\mathrm{pPO_3}$.

In this case, the experimental uncertainty of repeated measurements of type A was calculated using the formula:

$$u_A^2(\overline{pX}) = \frac{\sum_{i=1}^{m}(pX_i - \overline{pX})}{(m-1)m}\,, \tag{26}$$

where m is the number of measurement results [35], [42]-[50].

Considering the obtained values of experimental measurement uncertainties of type A (26), the type B uncertainty (25) caused by additive and multiplicative errors in the ion concentration measuring instrument, as well as the uncertainty due to nonlinearity error in the instrument (19), the value of the relative combined uncertainty in ion concentration measurement was calculated using the following formula:

$$\tilde{u}_C^2 = \left(\frac{u_{\mathrm{A}}(\overline{pX})}{|\overline{pX}|}\right)^2 + \left(\frac{u_{\mathrm{B}}}{|\overline{pX}|}\right)^2 + \delta_n^2\,. \tag{27}$$

Since, when performing the experiments, the deviation of the temperature of the object under study from the reference temperature value (20 °C) was $\Delta\eta$ = 2 K, and the permissible deviation of the ion concentration from the reference values was taken to be ΔpX =0.1 pX, then the uncertainty of type B caused by the existence of additive and multiplicative errors calculated using formula (25) was u_B = 25769 binary-decimal pulses. When converted to units of the measured quantity, the maximum value of type B uncertainty was $u_B = 7\ \mathrm{pX} \times 25769/(4.5 \times 10^6) = 0.04\ \mathrm{pX}$.

If we multiply the calculated values of the relative combined measurement uncertainty of ion concentration by 100 %, we can express the relative combined uncertainty as a percentage. By substituting the numerical values of the measurement uncertainties and the average value of ion concentrations into formula (27), we obtained the following values for the relative combined measurement uncertainty:

- for the concentration of fluoride ions

$$\tilde{u}_{\mathrm{C}}(pF) = \sqrt{\left(\frac{0.003}{3.013}\right)^2 + +\left(\frac{0.04}{3.013}\right)^2 + 0.017^2} \cdot 100\ \% = 2.16\ \%;$$

- for the concentration of potassium ions

$$\tilde{u}_{\mathrm{C}}(pK) = \sqrt{\left(\frac{0.0026}{1.905}\right)^2 + \left(\frac{0.04}{1.905}\right)^2 + 0.017^2} \cdot 100\ \% = 2.71\ \%;$$

- for the concentration of ammonium nitrogen ions

$$\tilde{u}_{\mathrm{C}}(pNH_4) = \sqrt{\left(\frac{0.0027}{5.345}\right)^2 + \left(\frac{0.04}{5.345}\right)^2 + 0.017^2} \cdot 100\ \% = 1.86\ \%;$$

- for the concentration of nitrate nitrogen ions

$$\tilde{u}_{\mathrm{C}}(pNO_3) = \sqrt{\left(\frac{0.0028}{3.15}\right)^2 + \left(\frac{0.04}{3.15}\right)^2 + 0.017^2} \cdot 100\ \% = 2.12\ \%;$$

- for the concentration of phosphate ions

$$\tilde{u}_{\mathrm{C}}(pPO_3) = \sqrt{\left(\frac{0.0039}{5.65}\right)^2 + \left(\frac{0.04}{5.65}\right)^2 + 0.017^2} \cdot 100\ \% = 1.84\ \%.$$

Based on the combined measurement uncertainty of ion concentrations, the expanded uncertainty values for each constituent element were calculated using the formula:

$$U = \pm\, k_{\mathrm{p}}\, \tilde{u}_{\mathrm{C}}\, \overline{pX}\,, \tag{28}$$

where k_{p} is the coverage coefficient for a normal distribution with probability p (for probability p = 95 % takes the value k_{p} = 1.96);

$\tilde{u}_C\,\overline{pX}=u_C$ is the absolute value of the combined uncertainty u_C, expressed through the relative combined uncertainty $\tilde{u}_C$ and the estimated value of the measured quantity $\overline{pX}$ ($\tilde{u}_C = u_C/\overline{pX}$) [34], [40], [43]-[50].

By substituting the estimated values of the constituent elements and their relative combined uncertainties into formula (28), the following values of expanded measurement uncertainties were obtained for a confidence level of p = 95 %:

$$U_{\mathrm{pF}} = \pm 1.96 \cdot 0.0216 \cdot 3.013 = \pm 0.128\ \mathrm{pF},$$

$$U_{\mathrm{pK}} = \pm 1.96 \cdot 0.0271 \cdot 1.905 = \pm 0.101\ \mathrm{pK},$$

$$U_{\mathrm{pNH_4}} = \pm 1.96 \cdot 0.0186 \cdot 5.345 = \pm 0.195\ \mathrm{pNH_4},$$

$$U_{\mathrm{pNO_3}} = \pm 1.96 \cdot 0.0212 \cdot 3.15 = \pm 0.131\ \mathrm{pNO_3},$$

$$U_{\mathrm{pPO_3}} = \pm 1.96 \cdot 0.0184 \cdot 5.65 = \pm 0.204\ \mathrm{pPO_3}.$$

Thus, the ion concentration measurement results can be expressed as follows:

$$\overline{pF} = 3.013 \pm 0.128\ \mathrm{pF\ at}\ p = 95\ \%,$$

$$\overline{pK} = 1.905 \pm 0.101\ \mathrm{pK\ \ at}\ p = 95\ \%,$$

$$\overline{pNH_4} = 5.345 \pm 0.195\ \mathrm{pNH_4\ at}\ p = 95\ \%,$$

$$\overline{pNO_3} = 3.15 \pm 0.131\ \mathrm{pNO_3\ at}\ p = 95\ \%,$$

$$\overline{pPO_3} = 5.65 \pm 0.204\ \mathrm{pPO_3\ \ at}\ p = 95\ \%.$$

The maximum expanded measurement uncertainty was ± 0.204 pX when measuring the concentration of phosphate ions (5.65 ± 0.204) $\mathrm{pPO_3}$, while the minimum expanded measurement uncertainty was ± 0.101 pX when measuring the concentration of potassium ions (1.905 ± 0.101) pK.

This demonstrates the feasibility of employing a model equation to determine the additive and multiplicative components of errors and incorporating these error components into the assessment of combined measurement uncertainty. The technique of recalculating additive and multiplicative errors into measurement uncertainty has been tested using the example of ion concentration measurements using a model equation of an ion concentration measuring instrument.

5. CONCLUSIONS

The paper presents metrological models that enable the analysis of the primary static characteristics of measurement instruments. These models are derived by expanding the transformation function of the measuring device into the Taylor series. The findings were validated using a measurement model that illustrates the conversion process from the input value (ion concentration) to the output binary-decimal code for a developed instrument designed to measure the concentrations of ion constituents in humus in soil using ion-selective electrodes. The technique was developed to account for additive and multiplicative error characteristics, enabling their conversion into a type B uncertainty component. This approach allows the research results to align with international standards, specifically ISO/IEC 17025, regarding the presentation of measurement accuracy. The proposed mathematical model for calculating type B measurement uncertainty utilizes influence coefficients (β_{0t}, β'_{0t}, and α_{0t}) that are instrumental in assessing the additive and multiplicative errors of the measuring device and are derived from the Taylor series terms. Consequently, applying this mathematical model yielded a type B measurement uncertainty value of u_B = 0.04 pX within the measurement range of 0.3 pX to 7 pX.

The results of the study on the expanded measurement uncertainty of ion concentrations in humus soil show that the values vary depending on the ion concentration range, ranging from ±0.101 pX when measuring at the lower concentration range of potassium ions 1.905 pX to ± 0.204 pX when measuring at the upper concentration range of phosphate ions 5.65 pX. These values consider uncertainties caused by additive and multiplicative errors, as well as nonlinearity errors.

REFERENCES

[1] P. Malhotra, Conductometric Methods. In: Analytical Chemistry. Springer, Cham, 2023. DOI: 10.1007/978-3-031-26757-4_11

[2] A. Abdelazim, M. Abourehab, L. Abd Elhalim, A. Almrasy, S. Ramzy, Different spectrophotometric methods for simultaneous determination of lesinurad and allopurinol in the new FDA approved pharmaceutical preparation; additional greenness evaluation, Spectrochimica Acta Part A: Molecular and Biomolecular Spectroscopy, Volume 285, 2023, 121868. DOI: 10.1016/j.saa.2022.121868

[3] G. G. Sadullayeva, Sh. B. Rakhmatov, Amperometric method of analysis and its advantages over other methods, International journal of research in commerce, IT, engineering and social sciences, 16(2), 2022, pp. 4–8. https://www.gejournal.net/index.php/IJRCIESS/article/view/244

[4] N. Carpenter, D. Pletcher, Amperometric method for the determination of nitrate in water, Analytica Chimica Acta, Volume 317, Issues 1–3, 1995, pp. 287-293. DOI: 10.1016/0003-2670(95)00384-3

[5] M. Mousavi, S. Sahari, N. Alizadeh, M. Shamsipur, Lead ion-selective membrane electrode based on 1,10-dibenzyl-1,10-diaza-18-crown-6, Analytica Chimica Acta, Volume 414, Issues 1–2, 2000, pp. 189-194. DOI: 10.1016/S0003-2670(00)00818-7

[6] O. Vasilevskyi, V. Sevastianov, K. Ovchynnykov, V. Didych, S. Burlaka, Accuracy of Potentiometric Methods for Measuring Ion Activity in Solutions. In: Yang, XS., Sherratt, S., Dey, N., Joshi, A. (eds) Proceedings of Seventh International Congress on Information and Communication Technology. Lecture Notes in Networks and Systems, vol 447, 2023. DOI: 10.1007/978-981-19-1607-6_16

[7] K. S. Barros, M. C. Martí-Calatayud, E. M. Ortega, V. Pérez-Herranz, and D. C. R. Espinosa, Chronopotentiometric study on the simultaneous transport of EDTA ionic species and hydroxyl ions through an anion-exchange membrane for electrodialysis applications, Journal of Electroanalytical Chemistry, vol. 879, 2020, p. 114782. DOI: 10.1016/j.jelechem.2020.114782

[8] L. Wang, W. Zhao, Damped least squares method for nonlinear mixed additive and multiplicative errors model, Measurement Science and Technology, 35(6), 2024, 066305. DOI: 10.1088/1361-6501/ad3391

[9] D. M. Rocke, S. Lorenzato, A Two-Component Model for Measurement Error in Analytical Chemistry, Technometrics, 37(2), 1995, pp. 176–184. DOI: 10.1080/00401706.1995.10484302

[10] Y. Tian, G. Huffman, R. Adler, L. Tang, M. Sapiano, V. Maggioni, H. Wu, Modeling errors in daily precipitation measurements: Additive or multiplicative, Geophysical Research Letters, 40(10), 2013, pp. 2060-2065. DOI: 10.1002/grl.50320

[11] O. Vasilevskyi, O. Voznyak, V. Didych, V. Sevastianov, O. Ruchka and V. Rykun, Methods for Constructing High-precision Potentiometric Measuring Instruments of Ion Activity, 2022

IEEE 41st International Conference on Electronics and Nanotechnology (ELNANO), Kyiv, Ukraine, 2022, pp. 247-252. DOI: 10.1109/ELNANO54667.2022.9927128

[12] Y. Kuang, A. Rajan, M. Ooi, S. Demidenko, Measured Quantity Value Estimator for Multiplicative Nonlinear Measurement Models, in IEEE Transactions on Instrumentation and Measurement, vol. 66, no. 4, 2017, pp. 715-722. DOI: 10.1109/TIM.2017.2658000

[13] R. P. Agarwal, K. Perera, and S. Pinelas, Taylor's Series, An Introduction to Complex Analysis, 2011, pp. 159–168. DOI: 10.1007/978-1-4614-0195-7_24

[14] R. Maex, On the Nernst-Planck equation, Journal of Integrative Neuroscience (JIN), 16(1), 2017, pp. 73-91. DOI: 10.3233/JIN-170008

[15] M. Jacobs, C. Lopez, A. Dobrynin, Quantifying the Effect of Multivalent Ions in Polyelectrolyte Solutions. Macromolecules, 54(20), 2021, 9577-9586. DOI: 10.1021/acs.macromol.1c01326

[16] Ö. Isildak and O. Özbek, Application of Potentiometric Sensors in Real Samples, Critical Reviews in Analytical Chemistry, vol. 51, no. 3, 2020, pp. 218–231. DOI: 10.1080/10408347.2019.1711013 http://dx.doi.org/10.2139/ssrn.3015752

[17] K. S. Barros, M. C. Martí-Calatayud, E. M. Ortega, V. Pérez-Herranz, D. C. R. Espinosa, Chronopotentiometric study on the simultaneous transport of EDTA ionic species and hydroxyl ions through an anion-exchange membrane for electrodialysis applications, Journal of Electroanalytical Chemistry, vol. 879, 2020, p. 114782. DOI: 10.1016/j.jelechem.2020.114782

[18] D. Berdat, H. Andres, S. Wunderli, Development of Suitable ISE Measurement Procedures for SI-Traceable Chemical Activity Determination, CHIMIA, vol. 63, no. 10, 2009, p. 670. DOI: 10.2533/chimia.2009.670

[19] J. Bockris, A. Reddy, Modern electrochemistry 2B: electrodics in chemistry, engineering, biology and environmental science, Springer Science & Business Media, 1998, 516 p. https://books.google.com/books?hl=ru&lr=&id=V3tpJrG1H5wC&oi=fnd&pg=PA1539&dq=Bockris,+J.O.+and+Reddy,+A.K.N.+(1970)+Modern+Electrochemistry.+Springer+US,+Boston.+10.1007/978-1-4615-7467-5&ots=OXtjQ_WukK&sig=T7fS3ho9mpMbmjm3xzBV0uXtT1k#v=onepage&q&f=false

[20] W. Nernst, Begründung der Theoretischen Chemie: Neun Abhandlungen, 2003, pp. 1889-1921, 1. Aufl. Verlag Harri Deutsch, Frankfurt am Main.

[21] J.O. Bockris, A.K.N. Reddy, Modern Electrochemistry, Springer US, Boston, 1970. DOI: 10.1007/978-1-4615-7467-5

[22] D. Pletcher, F. Walsh, Industrial electrochemistry, Springer Science & Business Media, 2012, 672 p. https://books.google.com/books?id=AnL7CAAAQBAJ&dq=D.+Pletcher,+%E2%80%9CIndustrial+Electrochemistry%E2%80%9D,+London:+Chapman+a.+Hall,+1982.&lr=&hl=ru&source=gbs_navlinks_s

[23] D. Pletcher, Industrial Electrochemistry, London: Chapman a. Hall, 1982.

[24] F. Scholz, Nikolsky's ion exchange theory versus Baucke's dissociation mechanism of the glass electrode, Journal of Solid State Electrochemistry, 15, 2011, pp. 67–68. DOI: 10.1007/s10008-010-1163-0

[25] O. Vasilevskyi, V. Didych, A. Kravchenko, M. Yakovlev, I. Andrikevych, D. Kompanets, Y. Danylyuk, W. Wójcik, A. Nurmakhambetov, Method of evaluating the level of confidence based on metrological risks for determining the coverage factor in the concept of uncertainty, Proc. SPIE 10808, Photonics Applications in Astronomy, Communications, Industry, and High-Energy Physics Experiments 2018, 108082C, 2018. DOI: 10.1117/12.2501576

[26] V. D. Bezuglyi, T. A. Khudyakova, A. M. Shkodin, Titrimetric methods for the analysis of non-aqueous solutions, 1986, 382 p.

[27] Oleksandr Vasilevskyi, Assessing the level of confidence for expressing extended uncertainty through control errors on the example of a model of a means of measuring ion activity, Acta IMEKO, vol. 10, no. 2, article 27, June 2021. DOI: 10.21014/acta_imeko.v10i2.810

[28] Single and Multichannel, Synchronous Voltage-to-Frequency Converters. https://www.analog.com/media/en/technical-documentation/data-sheets/AD7741.pdf

[29] M. Dalgobind, Engineering Metrology and Measurements, SSRN Electronic Journal, 2016. DOI: 10.2139/ssrn.3015752

[30] U. Pogliano, Evaluation of the uncertainties in the measurement of distorted power by means of the IEN sampling system, in IEEE Transactions on Instrumentation and Measurement, vol. 55, no. 2, pp. 620-624, 2006. DOI: 10.1109/TIM.2006.870129

[31] Carlos Mauricio Villamizar Mora, Jonathan Javier Duarte Franco, Victor Jose Manrique Moreno, Carlos Eduardo García Sánchez, Analysis of the mathematical modelling of a static expansion system, Acta IMEKO, vol. 10, no. 3, article 25, September 2021. DOI: 10.21014/acta_imeko.v10i3.1061

[32] M. Wegener, E. Schnieder, A Measurement Standard for Vehicle Localization and Its ISO-Compliant Measurement Uncertainty Evaluation, in IEEE Transactions on Instrumentation and Measurement, vol. 61, no. 11, pp. 3003-3013, Nov. 2012. DOI: 10.1109/TIM.2012.2203872

[33] A. Ferrero, S. Salicone, Fully Comprehensive Mathematical Approach to the Expression of Uncertainty in Measurement, IEEE Transactions on Instrumentation and Measurement, vol. 55, no. 3, pp. 706–712, Jun. 2006. DOI: 10.1109/tim.2006.873799

[34] Oleksandr Vasilevskyi, Maryna Koval, Svetlana Kravets, Indicators of reproducibility and suitability for assessing the quality of production services, Acta IMEKO, vol. 10, no. 4, article 11, December 2021. DOI: 10.21014/acta_imeko.v10i4.814

[35] BIPM, IEC, IFCC, ILAC, ISO, IUPAP, and OIML, Evaluation of measurement data − Guide to the expression of uncertainty in measurement, tech. rep., JCGM/WG1 GUM (2008). https://www.bipm.org/en/publications/guides

[36] ISO/IEC Guide 98-6:2021, Uncertainty of measurement - Part 6: Developing and using measurement models.

[37] ISO/IEC 17025:2017, General requirements for the competence of testing and calibration laboratories.

[38] O. Vasilevskyi, V. Didych, O. Zabula, V. Sarana, E. M. Popovici, Developing and using measurement models to assess accuracy: using the example of measurements of the activity of ions, 2023 IEEE International Conference on Industry 4.0, Artificial Intelligence, and Communications Technology (IAICT), BALI, Indonesia, 2023, pp. 125-129. DOI: 10.1109/IAICT59002.2023.10205656

[39] V. Ramnath, Determining the covariance matrix for a nonlinear implicit multivariate measurement equation uncertainty analysis. International Journal of Metrology and Quality Engineering, 13, 9, 2022. DOI: 10.1051/ijmqe/2022008

[40] O.M. Vasilevskyi, V.Yu. Kucheruk, E.T. Volodarskyi, Uncertainty of measurement, control and test results, Ukraine, Vinnytsia: VNTU, 2020, 352 p. ISBN 978-966-289-374-8.

[41] I. Farrance, R. Frenkel, Uncertainty of Measurement: A Review of the Rules for Calculating Uncertainty Components through Functional Relationships. Clin Biochem Rev, 2012, 33(2):49-75. https://pmc.ncbi.nlm.nih.gov/articles/PMC3387884.

[42] O. Kupriyanov, R. Trishch, D. Dichev, T. Bondarenko, Mathematic Model of the General Approach to Tolerance Control in Quality Assessment, Lecture Notes in Mechanical

Engineering, 2022, pp. 415–423. DOI: 10.1007/978-3-030-91327-4_41
[43] O. M. Vasilevskyi, V. M. Didych, Elements of the theory of construction of potentiometric means of measuring control of ion activity with increased reliability, Monograph, Ukraine, Vinnytsia: VNTU, 2013, 176 p. DOI: 10.13140/RG.2.2.35044.39044
[44] R. Trishch, O. Cherniak, D. Zdenek, V. Petraskevicius, Assessment of the occupational health and safety management system by qualimetric methods, Engineering Management in Production and Services, 2024, 16(2), pp. 118–127. DOI: 10.2478/emj-2024-0017
[45] A. A. Semenov, O. O. Semenova, O. M. Voznyak, O. M. Vasilevskyi, M. Y. Yakovlev, Routing in telecommunication networks using fuzzy logic, 2016 17th International Conference of Young Specialists on Micro/Nanotechnologies and Electron Devices (EDM), 2016, pp. 173-177. DOI: 10.1109/EDM.2016.7538719
[46] O. Kupriyanov, R. Trishch, D. Dichev, K. Kupriianova, A General Approach for Tolerance Control in Quality Assessment for Technology Quality Analysis, Lecture Notes in Mechanical Engineering, 2023, pp. 330–339. DOI: 10.1007/978-3-031-16651-8_31
[47] O. M. Vasilevskyi, P.I. Kulakov, Elements of the Theory of Accuracy Improvement in Measurement and Synchronization of Angular Velocities of Interconnected Electric Motor Rotors, Monograph, Ukraine, Vinnytsia: VNTU, 2011, 170 p. DOI: 10.13140/RG.2.2.19944.89606
[48] O. Cherniak, R. Trishch, R. Ginevičius, O. Nechuiviter, V. Burdeina, Methodology for Assessing the Processes of the Occupational Safety Management System Using Functional Dependencies, Lecture Notes in Networks and Systems, 2024, 996 LNNS, pp. 3–13. DOI: 10.1007/978-3-031-60549-9_1
[49] O. M. Vasilevskyi, Advanced mathematical model of measuring the starting torque motors, Technical Electrodynamics, 2013, (6), pp. 76–81. DOI: 10.13140/RG.2.1.4376.9044
[50] R. Trishch, O. Nechuiviter, H. Hrinchenko, M. Riabchykov, I. Pandova, Assessment of safety risks using qualimetric methods, MM Science Journal, 2023, 2023(10), pp. 6668–6674. DOI: 10.17973/MMSJ.2023_10_2023021